Research on Scheme Design and Structure Optimization of High Speed and High Precision Vehicle Contour Detection Platform

Nutao Zhang[*,1, a], Qingping Bai[1,b], Bo Huang[2,c], and Qian Zhou[3,d]

[1]China Automotive Engineering Research Institute Co, Ltd, China;

[2]Chong Qing CAERI Test Equipment Co, Ltd, China;

[3]College of Artificial Intelligence, Southwest University, China.

[a]zhangnutao@caeri.com.cn, [b]baiqingping@caeri.com.cn, [c]huangbo1@caeri.com.cn, [d] swuzhq@sina.com.

Abstract. To improve road traffic safety and reduce the incidence of unauthorized vehicle modifications, overloading, and oversizing, this study proposed a detection platform structure to support the quick measurement of key dimensions and high-precision reconstruction of local features using the automotive contour size system. Using CAE technology, static and dynamic characteristic analysis was performed on the platform structure, and optimization design was conducted on the column frame and gantry frame separately. The optimized column frame's first-order modal frequency increased by 243% from 5.16 Hz to 17.65 Hz, with an average optimization ratio of 187% for the first six modal frequencies. For the optimized gantry frame, the average optimization ratio of the key node displacement exceeded 46%, with the first-order modal frequency increasing by 13% from 36.43 Hz to 41.33 Hz, and an average optimization ratio of 21% for the first six modal frequencies. Ultimately, the optimized detection platform's key nodes achieved an average optimization ratio of nearly 60%, with the first-order modal frequency increasing by 240% from 5.16 Hz to 17.57 Hz and an average optimization ratio of 185% for the first six modal frequencies. The optimized platform structure provides robust support for the high-speed and high-precision vehicle contour detection system's implementation.

Keywords: Vehicle; Detection platform; Design; CAE; Structure Optimization.

1. Introduction

As commercial vehicle ownership continues to increase, the economic losses caused by traffic accidents are also increasing[1]. In order to improve road traffic safety, effectively curb unauthorized vehicle modifications, and significantly reduce overloading and oversize phenomena, it is necessary to implement mandatory and periodic fast and accurate contour detection of commercial vehicles, especially trucks[2]. In the past, many inspection agencies used manual methods to measure the parameters of the vehicle's external dimensions, typically using tools such as calipers and lead hammers. This method is time-consuming, laborious, and inefficient, and the measurement accuracy is highly subject to human subjectivity[3]. In recent years, some researchers have been dedicated to developing automatic external dimension detection systems, but they usually only measure the length, width, and height dimensions of the vehicle, and cannot generate a true 3D model of the vehicle. At the same time, they cannot detect critical parts that affect transportation safety, such as the box body, safety fence, and tank body of the vehicle[4]. To address these challenges, our team has developed an intelligent vehicle contour size detection system that enables fast measurement of key vehicle dimensions and high-precision reconstruction of local features. This system is based on sensor and visual technologies, and multiple types and quantities of sensors and cameras are placed at specific detection locations to perform targeted data collection and analysis on vehicles entering the detection area. Typically, these sensors and cameras are installed on fixed or movable support platforms according to actual needs. In order to ensure stable operation of the sensors and cameras and reliable data, it is important to design the structure of the platform reasonably and explore and optimize its static and dynamic performance, thus avoiding large displacements and vibrations in the data acquisition location.

The CAE (Computer Aided Engineering) technology is an application technique that utilizes finite element methods to obtain parameters such as structural deformation, stress, natural frequency, and vibration mode. It can also achieve structural lightweighting and topology optimization in a wide range of applications such as aerospace, automotive, mechanical, civil, and biomedical engineering[5–8]. In the known literature on bracket-type structures, Zheng et al.[9] used CAE technology to conduct static analysis and optimization research on contour measuring brackets, improving the overall static performance of the brackets. Lou et al.[10] designed and developed a contour measuring instrument for measuring gantry structures and used CAE technology to analyze the dynamic characteristics of the gantry structure, obtaining a better dynamic structural scheme. Tian et al.[11] designed a support-type self-elevating platform for offshore oil and gas exploration, construction, and offshore wind farms, and used CAE technology to perform modal analysis and topology optimization on the support structure, ultimately obtaining a lighter weight support structure with better ultimate bearing capacity and dynamic response. Jia et al.[12] used topology optimization to design and develop a folding protective cover with a supporting framework, and ultimately proved its impact resistance performance through ballistic experiments. Similarly, Sun et al.[13] used topology optimization methods to optimize the design of bracket-type thin-walled structures, obtaining an optimized distribution of easy-to-manufacture reinforcing rib structures. The above studies all applied CAE technology to solve structural problems of bracket-type platforms, providing reference and efficient research ideas and methods for the special functional requirements of this study.

In this work, the main objective is to develop a vehicle contour detection platform structure that can support the rapid measurement of critical dimensions and high-precision reconstruction of local features, with a focus on ensuring the platform's good static and dynamic performance. Firstly, a functional analysis was conducted on the vehicle contour detection system for rapid measurement of critical dimensions and high-precision reconstruction of local features, which was developed by the team in the previous stage. Subsequently, a movable gantry-type support platform that matches the function of the detection system was designed. The static and dynamic characteristics of the platform structure were analyzed using CAE technology, examining the displacement deformation of key positions such as sensors and cameras as well as the dynamic characteristics of the entire support structure, and weak links in the platform structure were identified. According to the simulation results, empirical design method and topology optimization method were used to optimize the weak structure. Finally, the optimized platform structure's static and dynamic performance indicators were compared with those of the original design structure, proving the outstanding performance advantages of the optimized structure and providing strong support for the realization of the high-speed and high-precision vehicle contour detection system.

2. Scheme design

2.1 Functional scheme design

The vehicle contour detection system developed in the initial stages of development, which involves the rapid measurement of key vehicle dimensions and high-precision reconstruction of local features, consists of two main components. Firstly, it employs an organic combination of non-contact sensors to achieve rapid measurement of key vehicle dimensions, enabling more efficient road detection operations. Secondly, a visual system is utilized to achieve high-precision reconstruction of local vehicle features, thereby facilitating an evaluation of the compliance of key vehicle areas with traffic regulations. The key dimensions requiring inspection were determined based on actual needs, including the maximum length, maximum width, maximum height, wheelbase, and wheel spacing. The camera + lidar visual system combination was selected for realizing local feature 3D reconstruction, and was arranged around the vehicle. The specific configuration of the sensor and visual system combination is presented in Table 1.

Table 1. Detection system scheme

Scheme category	Functional attribute	Detection index	Configuration scheme
Non-contact sensor	High speed detection	Maximum vehicle length	Safety light screen
		Maximum vehicle width	Direct laser sensor
		Maximum vehicle height	Opposite-beam laser sensor
Visual system	High precision detection	Wheelbase	Ultrasonic sensor
		wheel spacing	Ultrasonic sensor
		Local 3D feature	camera + lidar

2.2 Structural scheme design

Based on the functional scheme, we have developed a platform structure scheme to support the entire detection system, as depicted in Figure 1. To cater to the detection of large commercial vehicles, our platform design features dimensions of 18000 mm × 2600 mm × 4100 mm. To ensure high-speed data acquisition of key dimensions, we adopted a gantry frame structure to carry the entire detection system. A safety light screen installed at the bottom of the fast-moving gantry frame detects the vehicle length, and the maximum length of the vehicle can be acquired after a single scan. The direct laser sensors, located on both sides of the bottom of the movable gantry frame, detect the vehicle width by moving quickly through the guide slide mechanism at the bottom of the gantry frame, and then extract the maximum width of the vehicle. The laser sensor for detecting vehicle height is located at the entrance of the vehicle on top of the column, which quickly collects the maximum size of the vehicle height upon entering the detection area. In addition, the ultrasonic sensor, located at the bottom of the column at the entrance of the vehicle, detects the wheelbase and wheel spacing, and their dimensional data can be acquired after the vehicle enters the detection area. For high-precision local feature data acquisition, we deployed 9 sets of camera + lidar vision systems in the middle of each column and gantry frame. These visual data are selected and extracted organically based on the detection requirements and the actual vehicle situation. Finally, we employed the dynamic + static layout of the platform structure scheme to achieve data acquisition of the detection system.

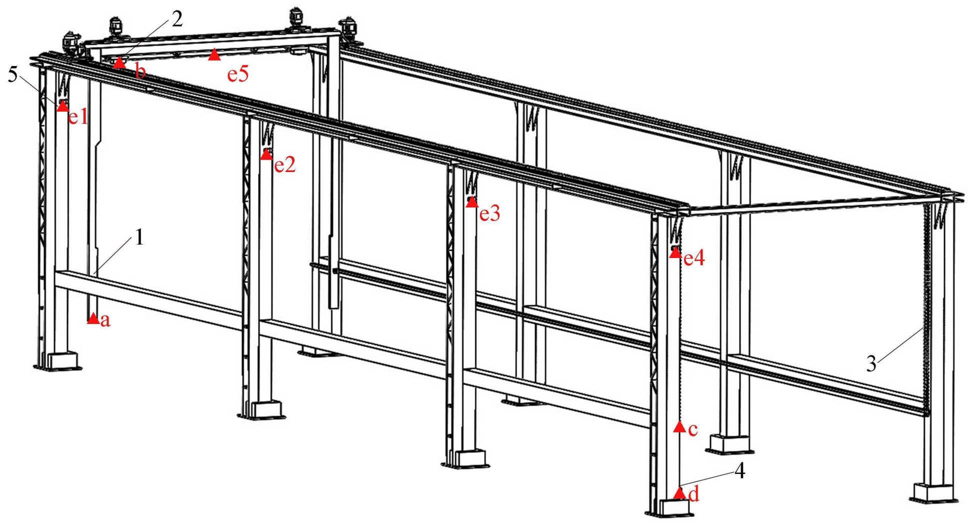

Fig. 1 Test platform design scheme: 1. safety light screen, 2. direct laser sensor, 3. opposite-beam laser sensor, 4. ultrasonic sensor (2 groups), 5. camera + lidar (9 groups).

2.3 Platform structure requirement analysis

In order to ensure the acquisition of high-quality vehicle data, it is crucial to construct a detection platform with sound structural characteristics. This requires that the installation of sensors and vision systems on the platform's support structure should not lead to significant deformation or vibration. Additionally, the fast-moving gantry structure should possess excellent dynamic characteristics to ensure that the sensors placed on it are not subject to large deformations or vibrations. In light of these requirements, this study employs CAE technology to conduct static and overall modal analyses on the entire support platform under extreme working conditions. This analysis aims to investigate the static displacement and dynamic characteristics of key positions of each sensor. Specifically, the study focuses on monitoring the displacement data of each sensor position, as illustrated in Figure 1. Given that the entire platform is symmetrical, 8 monitoring nodes (a-e) have been selected for this purpose. Furthermore, the study examines the modal data of the entire gantry frame structure to gain insight into its dynamic behavior.

3. Finite element analysis of platform structure

3.1 Basic finite element theory

3.1.1 Basic idea

The finite element method (FEM) is a numerical technique that discretizes a continuous structure into small elements. The elements are interconnected by nodes to form a complete model. By establishing the equations of each element and combining the load and boundary conditions, the equations for the entire structure can be constructed and solved. The FEM process consists of four steps: model discretization, unit analysis, whole analysis, and numerical solution[14].

3.1.2 Mathematical model

After discretizing an actual structure using the finite element method, the dynamic differential equation can be written as[14]:

$$[M]\ddot{x} + [C]\dot{x} + [K]x = F(t) \tag{1}$$

Where, [M], [C] and [K] are the mass matrix, damping matrix and stiffness matrix respectively; $\ddot{x}$, $\dot{x}$ and x are the node acceleration, velocity and displacement vector respectively; $F(t)$ is the load vector.

For static analysis, the load is a constant that does not vary with time, so equation (1) can be simplified to:

$$[K]x = F \tag{2}$$

Modal analysis is primarily used to identify the modal parameters of linear system structures, which describe independent equations in terms of modal coordinates and modal parameters. For modal analysis, the modal properties are intrinsic to the structure and independent of external excitations, and damping has little effect on the natural frequency. Therefore, the dynamic equation can be simplified to:

$$[M]\ddot{x} + [K]x = 0 \tag{3}$$

The equation can be transformed into an eigenvalue equation:

$$\left([K] - \omega^2 [M]\right)\varphi = 0 \tag{4}$$

Where, ω is the circular frequency, namely the characteristic value, rad/s; φ is the mode shape, that is, the eigenvector. The modal analysis is essentially the eigenvalue analysis.

3.2 Model building

3.2.1 Finite element model

To enhance the efficiency of the simulation analysis, the geometric model of the entire platform structure was simplified first. This simplification involved removing all the small features such as fillets, chamfers, and small holes, as strength analysis was not being considered. The geometric structures of the guide rail slider, rack, and some complex components were regularized. Additionally, the motor reducer was treated as a concentrated mass. Subsequently, the simplified platform structure was imported into the Hypermesh software to establish a finite element model. The plate parts, such as the column and gantry, were divided into 2D quadrilateral meshes, while the block-shaped components, such as the guide rail slider and slide pad, were divided into 3D hexahedral meshes. After welding and contact treatment were applied to each component, a structured mesh with the correct assembly relationship was obtained, as shown in Figure 2. The assembly mesh had a total of 1,334,896 nodes and 1,010,934 elements. The Jacobian values of the quadrilateral and hexahedral elements > 0.7, and the mesh quality was satisfactory.

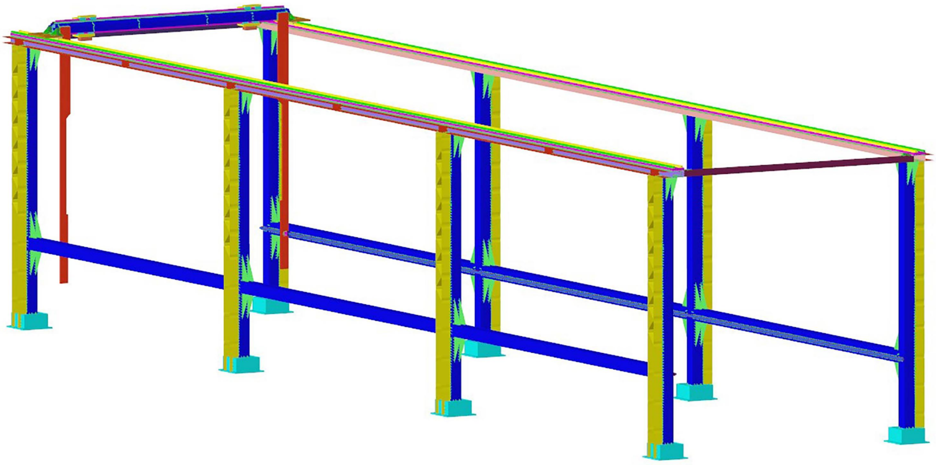

Fig. 2 Mesh of platform structure.

3.2.2 Constraints and analysis Settings

Static analysis involved imposing fixed constraints on the bottom plates of each base of the platform structure to limit movement degrees of freedom in three directions. To simulate the ultimate operating condition of the gantry frame, the gantry frame was placed in the initial position, and a force equivalent to 1.5g of inertia load (7520 N) was applied to the rack and pinion drive node below the gantry slide, and a force equivalent to 1.5g of inertia load (1300 N) was applied to the rack and pinion drive node on the side of the slide seat assembly of the measured width. For modal analysis, the constrained operating conditions of each bottom plate were taken into account, and the Lanczos Iteration Method was employed to solve the modal eigenvalues.

The material properties of each part are provided in Table 2. Specifically, the base, column, and gantry frame were constructed using Q235, the slide seat using ZL114A-T6, the guide rail using 55 steel, the slide block using 15CrMo, and the rack and pinion using SNCM220.

Table 2. Material parameters of parts

Component	Material	Modulus of elasticity /MPa	Poisson's ratio	Density /t/mm^3
Base Column Gantry frame	Q235	212000	0.288	7.86e-9
Slide seat	ZL114A-T6	70000	0.3	2.7e-9
slider	15CrMo	212000	0.284	7.88e-9
Guide rail	55	217000	0.27	7.83e-9
Rack and pinion	SNCM220	208000	0.295	7.87e-9

3.3 Result analysis

3.3.1 Statics results

The static deformation cloud map of the platform structure is presented in Figure 3. The figure shows that the main deformation area of the entire platform is concentrated in the upper region, especially between each vertical column, where the deformation is larger. The maximum displacement occurs at the end of the safety light curtain, primarily due to the insufficient structural stiffness of the light curtain hanger and guiding support. Additionally, the local stiffness in the middle of the gantry is also poor, which could lead to significant vibrational deformation during operation.

Further processing of displacement data from sensor nodes was obtained, and the results are shown in Table 3. The table reveals that the largest displacement occurs at the visual sensor node in the lower-middle part of the gantry, with a value of 0.384 mm, followed by the laser sensor nodes on the left and right sides of the gantry, with a value of 0.241 mm. These displacements may have a significant impact on the stability and accuracy of the gantry's operation. Another notable displacement occurs at the laser sensor node below the safety light curtain, with a value of 0.235 mm, which may also significantly affect the accuracy of the safety light curtain. The displacements at other locations are relatively small, ensuring the normal and stable operation of the sensors. Therefore, the stiffness of the gantry structure and the surrounding safety light curtain structure needs to be strengthened.

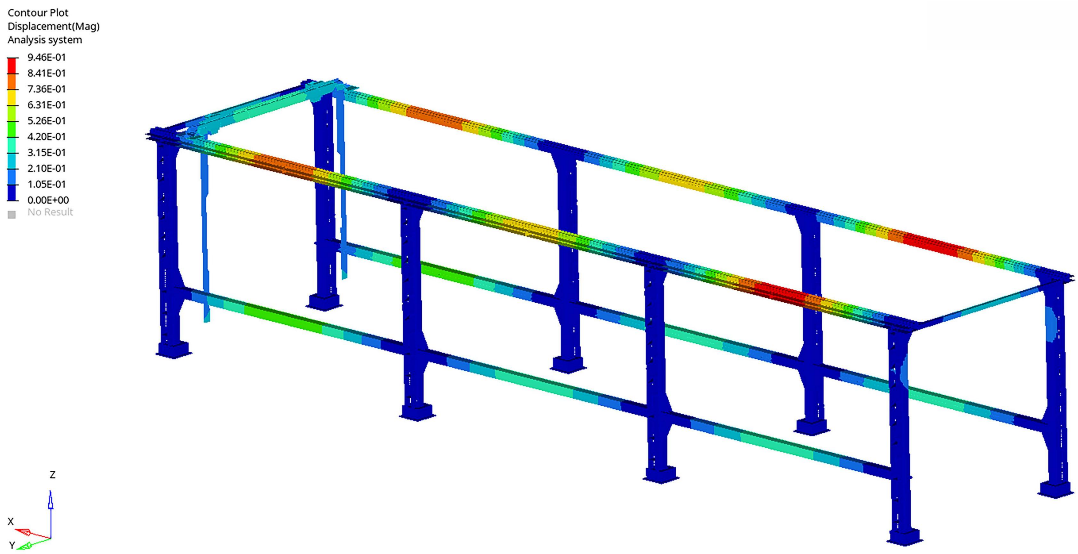

Fig. 3 Displacement of platform

Table 3. Displacement of critical positions

Location	X-deformation/mm	Y-deformation/mm	Z-deformation/mm	Total deformation/mm
a	0.114	0.106	0.176	0.235
b	0.058	0.028	0.231	0.241
c	0.013	0.001	0.007	0.015
d	0	0	0.003	0.003
e1	0.022	0.007	0.019	0.030
e2	0.031	0.022	0.022	0.044
e3	0.017	0.063	0.025	0.070
e4	0.101	0.007	0.009	0.102
e5	0.103	0.003	0.370	0.384

3.3.2 Modal results

The modal analysis results are presented in Figure 4 and Table 4. Based on the figure, it can be observed that the vibration mode of the platform is not localized to a specific structure, but rather to the entire support system. The modal vibration modes are primarily concentrated in the first-order bending and torsion modes along the vertical columns of the platform. This indicates that the weak points of the support system are mainly concentrated on the vertical columns. The table reveals that the modal frequencies of the first six modes are all below 10 Hz, which is not ideal. This could result in the platform being easily excited by low-frequency vibrations from vehicles and roads during the inspection process, causing large vibration displacements and even resonance.

Due to the large operating range of the platform, the preliminary design of the support structure was relatively long, leading to overall bending and torsion. Therefore, it is necessary to strengthen the support structure at various locations on the platform to improve its dynamic stiffness.

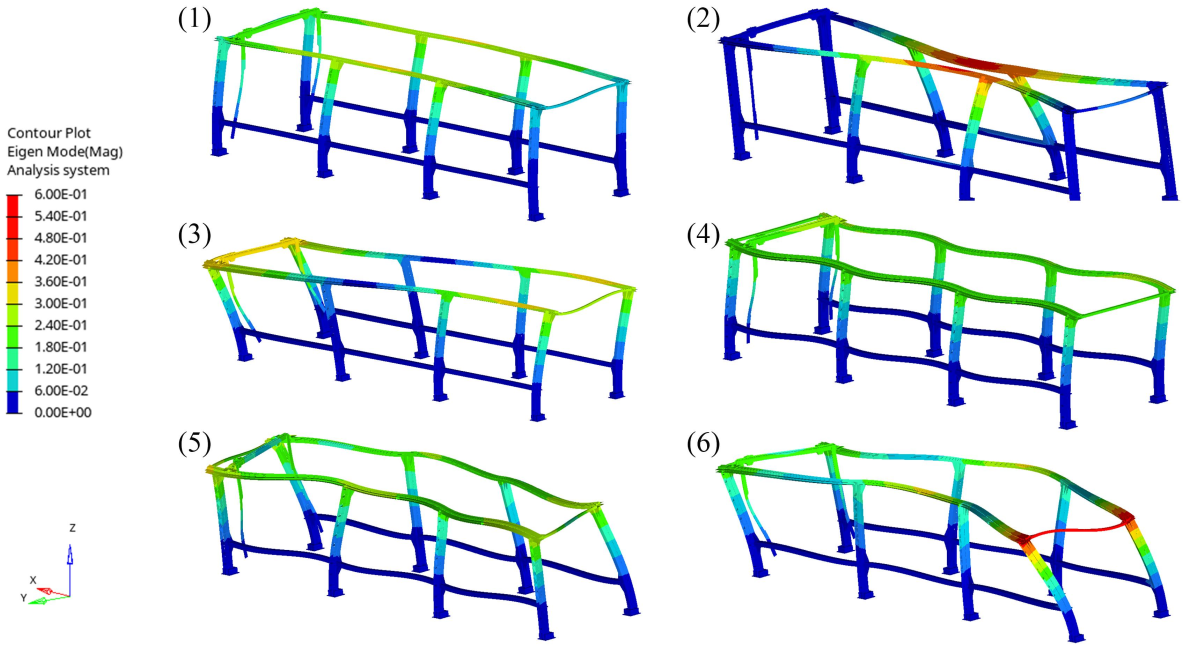

Fig. 4 mode shape of platform: the serial number represents the mode order

Table 4. Modal frequencies and shapes of the first 6 orders

Modal order	Modal frequency /Hz	Mode shape
1	5.16	First-order bending of the platform along the Y-direction
2	5.93	First-order torsion in the middle part of the platform truss along the Y-direction
3	6.10	First-order torsion of the platform along the Y-direction
4	6.92	First-order bending of the platform along the X-direction
5	7.58	First-order torsion of the platform along the z-axis
6	8.35	Second-order torsion of the platform along the y-direction

4. Structure optimization

Based on the findings above, it is evident that the overall platform structure lacks satisfactory levels of both static and dynamic stiffness. As a result, there is a need to undertake structural optimization work to enhance the platform's structural performance. This optimization work is predominantly divided into two components. Firstly, a comprehensive approach is required to redesign and fortify the deficient links of the column frame. This approach will be based on the modal analysis results and will aim to enhance the modal frequency of the support structure while minimizing deformation in critical locations. The second component involves utilizing the topology optimization method to enhance the structural performance of the moving gantry. This will entail a focus on improving the overall stiffness of the gantry, particularly in key locations, while achieving maximal weight reduction. Ultimately, the static and dynamic characteristics of the whole platform will be explored.

4.1 Optimization design of column frame

In light of the potential weak links in the column frame, a comprehensive approach to structural strengthening has been undertaken. This approach has been executed through the implementation of the following measures:

1. A uniform encryption design has been implemented for the column frame to minimize deformation in the mid-section of the upper and lower guide truss frame.
2. A support group has been installed around the entire column frame to mitigate low-order vibrations in both the front-to-rear and left-to-right directions, thereby enhancing the dynamic characteristics of the entire platform.
3. Double-row triangular rib plates have been added to the connections of each stent to enhance the local stiffness of the stent connections.
4. Safety light curtain moving tracks have been introduced on both the left and right sides of the platform to bolster the local stiffness of the safety light curtain installation plate.

The structure of the column frame after optimized design is shown in Figure 5.

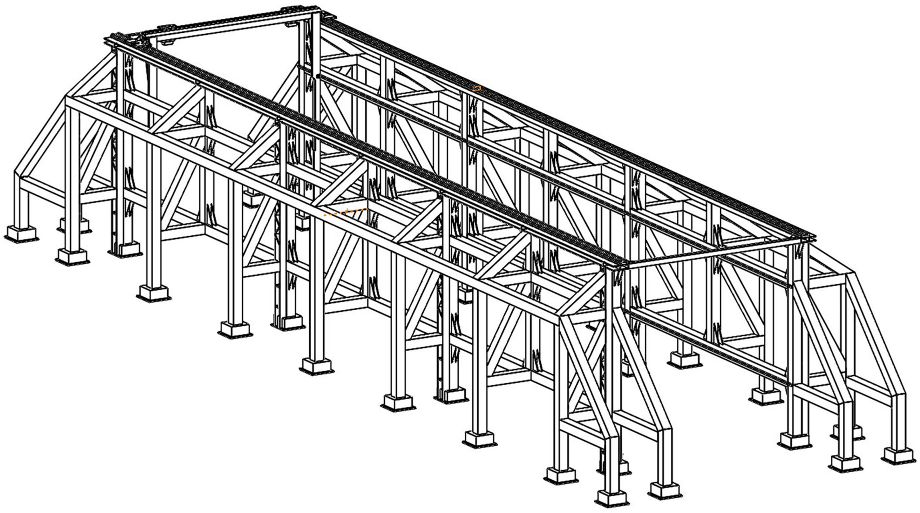

Fig. 5 Optimized design of column frame structure

4.2 Topology optimization of gantry frame

Due to the lack of local stiffness in the middle of gantry frame during the high acceleration operation, the topology optimization of gantry structure was carried out especially with the goal of minimizing the flexibility.

4.2.1 Mathematical model

This work is done in Optistruct, where the goal of topology optimization is to minimize compliance. Assuming the material density in the design domain is $\rho(x)$ in the design domain Ω, the flexibility formula of the object can be obtained based on the fundamental principles of material mechanics as follows[15]:

$$U(\rho) = 21\int \Omega\rho(x)uT(x)K(x)u(x)dx \tag{5}$$

Where, $u(x)$ is the node displacement vector, $K(x)$ is the stiffness matrix and $\rho(x)$ is the material density. The material density was converted into a continuous variable $\overline{\rho}(x)$ between 0 and 1, and the Heaviside function $H(\overline{\rho})$ is used to discretize the continuous variable, which can be written as:

$$\rho(x) = H(\overline{\rho}(x)) = \begin{cases} 1 & \overline{\rho}(x) > 0.5 \\ 0 & \overline{\rho}(x) < 0.5 \end{cases} \tag{6}$$

Where, $H(\overline{\rho})$ is defined as :

$$H(\overline{\rho}) = \begin{cases} 0 & \overline{\rho} < 0 \\ \overline{\rho} & 0 \le \overline{\rho} \le 1 \\ 1 & \overline{\rho} > 1 \end{cases} \tag{7}$$

To transform the optimization problem into an unconstrained one, the Solid Isotropic Material with Penalization (SIMP) method is adopted to penalize the material density[16], resulting in the optimization objective:

$$\min_{\overline{\rho}} \left[\frac{1}{2} \int_{\Omega} H(\overline{\rho}(x)) u^T(x) K(x) u(x) dx + \beta \int_{\Omega} \overline{\rho}(x)^p dx \right] \tag{8}$$

Where, β is a constant, p is a penalty factor, and is taken as 3[17, 18] by referring to the studies of various literatures. According to the Karush-Kuhn-Tucker (KKT) condition, the updated formula can be obtained as follows:

$$\overline{\rho}^{k+1}(x) = \max\left(0, \max\left(-\psi(y,x)\right)\right), y \in [0,1] \tag{9}$$

Where, $\psi(y,x)$ is Lagrange multiplier, which can be obtained through sensitivity analysis:

$$\psi(y,x) = \frac{\partial U}{\partial \overline{\rho}} - \beta p y^{p-1} \tag{10}$$

Finally, a mathematical programming method is employed to optimize the material density through a series of iterations until the final optimal solution is obtained.

4.2.2 Model building and parameter setting

This topology optimization study is limited to the gantry frame and its auxiliary connection structure. The finite element model was established using the same strategy as described above, with the exception of modifying the structural thickness inward filling and mesh encryption of the gantry frame. The load condition was consistent with those previously defined, and the connection surface with the column frame was set as a fixed constraint condition.

The design space was defined as the gantry structure with the connecting part removed, while the rest was defined as the non-design space. The optimization objective was to minimize the global compliance of the gantry frame, subject to a first order frequency constraint greater than 42 Hz, a second order frequency constraint greater than 50 Hz (slightly above the modal frequency of the original structure), and a volume constraint between 0% and 20% of the original volume. Additionally, fabrication constraints included the symmetry constraint of the gantry frame in the XZ plane and a minimum size constraint of 20 mm to maintain a significant stiffness path.

4.2.3 Topology results and model reconstruction

After 35 iterations, convergence was achieved, and the topology of the gantry structure was obtained, as shown in Figure 6(a). The figure illustrates that the gantry structure after optimization is left-right symmetrical, with the removal of mass from multiple areas along the left and right edges as well as the middle section. The optimized structure retains a clear lattice-like path structure, exhibiting distinct topological features.

Considering factors such as manufacturability and cost control, the primary stiffness path transfer structure was retained during the reconstruction and design of the gantry topology. A design approach that emphasized uniformity and symmetry was adopted, leading to the final optimized gantry structure depicted in Figure 6(b).

(a)

(b)

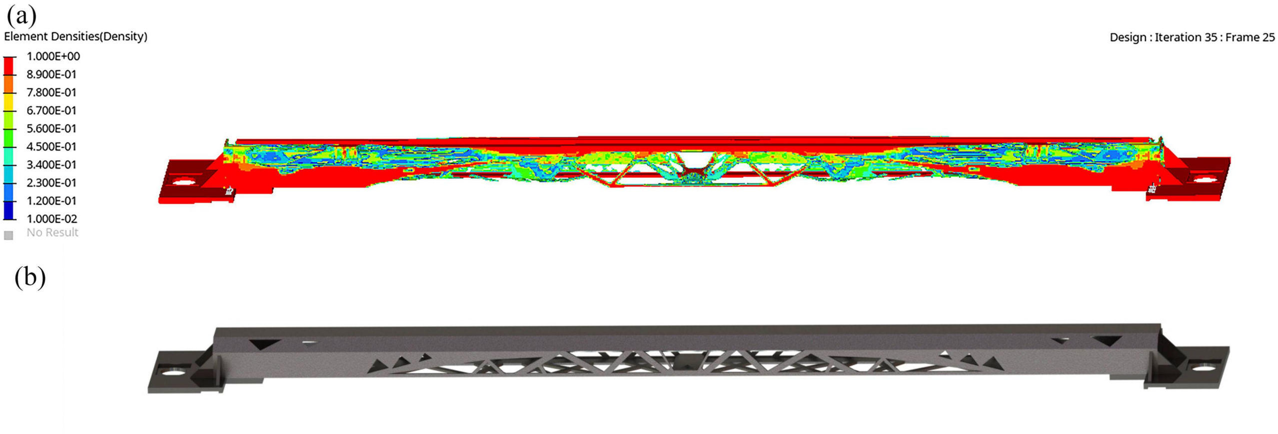

Fig. 6 Topological morphology and reconstruction structure of gantry frame

4.3 Model analysis and comparison

The various components and the overall structure of the above platform were simulated and analyzed and compared to explore the specific optimization effect.

4.3.1 Comparison of structural characteristics of column frame

The CAE analysis of the separate column frame structures before and after optimization was carried out using the same methods and conditions, and the low-order mode frequency data were obtained, as shown in Table 6. As can be seen from the table, compared with the column frame before optimization, the first mode frequency of the optimized column frame increased from 5.16 Hz to 17.65 Hz, and the optimization ratio reached 243%. The first six mode frequencies were greatly improved, and the average optimization ratio reached 187%. The optimized design of the column frame has a good effect, which is conducive to improving the overall dynamic stiffness of the platform.

Table 6. Comparison of optimization results of column frame

State	Frequency /Hz					
	1	2	3	4	5	6
Before optimization	5.16	5.48	6.30	7.11	7.49	8.51
After optimization	17.65	17.81	18.46	19.37	19.47	19.58
Optimization percentage	243%	225%	193%	172%	160%	130%

4.3.2 Comparison of structural characteristics of gantry frame

Using the same methods and conditions, CAE analysis was performed on the optimized and unoptimized gantry structures separately, and the displacement data of the nodes with large deformation and the low-order modal frequency data on the gantry were obtained, as shown in Table 7. It can be seen from the table that the optimized gantry has significantly improved key node displacements compared to the unoptimized gantry, with an average optimization ratio of over 46%. In addition, the first-order modal frequency has increased from 36.43 Hz to 41.33 Hz, with an optimization ratio of 13%, and the first six modal frequencies have been improved to a certain extent, with an average optimization ratio of 21%. This indicates that the topological optimization of the gantry was effective in improving its overall static and dynamic stiffness.

Table 7. Comparison of optimization results of gantry frame

State	Displacement /mm		Frequency /Hz					
	b	e5	1	2	3	4	5	6
Before optimization	0.111	0.321	36.43	41.34	41.59	48.65	57.09	71.16
After optimization	0.063	0.161	41.33	41.38	48.96	69.95	76.90	78.55
Optimization percentage	43%	50%	13%	0%	18%	44%	35%	10%

4.3.3 Comparison of structural characteristics of platform

The identical method and conditions were employed to conduct CAE analysis on the entire platform structure prior to and post-optimization. Subsequently, displacement data and low-order modal frequency data of nodes with significant deformation were obtained and presented in Table 8. The table indicates that the optimized platform has effectively improved the displacement of key nodes when compared to the platform prior to optimization. The average optimization ratio of key nodes is approximately 60%. Additionally, the frequency of the first mode was increased by 17.57Hz from 5.16Hz, and the optimization ratio reached 240%. Moreover, the frequencies of the first six modes were also greatly improved, and the average optimization ratio reached 185%. These enhancements ensure the effective functioning of sensors at each location, enhance the dynamic stiffness of local positions, and aid in resisting external low-frequency vibration. In conclusion, the design and optimization of the testing platform structure were successful.

Table 8. Comparison of optimization results of platform

State	Displacement /mm			Frequency /Hz					
	a	b	e5	1	2	3	4	5	6
Before optimization	0.235	0.241	0.384	5.16	5.93	6.10	6.92	7.58	8.35
After optimization	0.058	0.103	0.206	17.57	17.90	18.16	19.13	19.45	19.77
Optimization percentage	75%	57%	46%	240%	202%	198%	176%	157%	137%

5. Summary

In this paper, a detection platform was designed to support the rapid measurement of vehicle key dimensions and the high precision reconstruction of local features to realize the function of the vehicle contour size system. CAE technology was applied to analyze the static and dynamic characteristics of the platform structure, and various weak links of the platform were optimized, and the following conclusions were obtained:

1. Based on the functional requirements of the vehicle contour size system for rapid measurement of vehicle key dimensions and high precision reconstruction of local features, the scheme and structure design of the moving gantry frame type detection platform were carried out. The static analysis and modal analysis of the preliminary design of the platform structure were carried out through CAE technology, and various weak links of the platform structure were explored.

2. Based on the results of static analysis and modal analysis, the optimized design of the platform column frame was carried out. Compared with the column frame before optimization, the first-order modal frequency of the optimized column frame was increased from 5.16 Hz to 17.65 Hz, and the optimization ratio reached 243%. It is beneficial to improve the overall dynamic stiffness of the platform.

3. Based on the results of static analysis and modal analysis, topology optimization was carried out on the gantry frame of the platform. Compared with the gantry frame before optimization, the average optimization ratio of key node displacement of the optimized gantry was more than 46%,

the first-order modal frequency was increased from 36.43 Hz to 41.33 Hz, and the optimization ratio was 13%. The frequencies of the first 6 modes are all increased to a certain extent, with an average optimization ratio of 21%. The topologically optimized gantry frame has better static and dynamic stiffness.

4. The displacement of key nodes and low-order modal frequency data of the platform structure before and after optimization are compared. Compared with the pre-optimization platform, the displacement of the optimized platform at key nodes has been effectively improved, the average optimization ratio of key nodes is close to 60%, the first-order modal frequency increases from 5.16 Hz to 17.57 Hz, and the optimization ratio reaches 240%. Moreover, the first 6 modes also have a great increase in frequency, with an average optimization ratio of 185%. The design and optimization of the detection platform structure is successful.

Acknowledgments

The work was founded by Application Innovation and Technology Development Foundation of Chongqing City of China (cstc2021jscx-gksbX0041).

References

[1] Hu Siran, Zhou Bowen, Zhang Tianyu. Spatio-temporal Analysis of Oversize-Overweight (OSOW) Vehicle based on Transportation Big Data[J]. Highway, 2020, 65 (8): 349-359.

[2] Zhang Wenhui, Guan Qiang, Sun Fengying, et al. Identification of geometric dimensions exceeding the limit when loading highway transportation vehicles[J]. Journal of Northeast Forestry University, 2009, 37 (4): 108-111.

[3] Gao Jingang, Liu Zhiyong, Zhang Shuang, et al. Application of binocular stereo vision technology in key dimension detection of CRH body[J]. Journal of Computer Applications, 2018, 38 (9): 2673-2677+2719

[4] Jiang Qingchang, Wang Dong, and Shi Wangyuan. Development of Vehicle body Dimensions Machine Based on Photoelectric Following and Laser Measurement Technology[J]. Journal of mechanical Engineer, 2008 (5): 79-80.

[5] Zhang Zixin, Jiang Liming, Yarlagadda Tejeswar, et al. OPS-ITO: Development of Isogeometric Analysis and Topology Optimization in OpenSEES for free-form structural design[J]. Computer-Aided Design, 2023: 103517.

[6] Zhu Jihong, Zhang Weihong, Xia Liang. Topology Optimization in Aircraft and Aerospace Structures Design[J]. Archives of Computational Methods in Engineering, 2016, 23(4): 595–622.

[7] Zhou Chenbo, Xia Mingyi, Xu Zhenbang. Design and optimization of a quadrupedal dynamic disturbance force measurement platform using strain gauges[J]. Mechanical Systems and Signal Processing, 2023, 188: 110032.

[8] Yüksel Esra, Budak Erhan, Ertürk Ahmet S. The Effect of Linear Guide Representation for Topology Optimization of a Five-axis Milling Machine[J]. Procedia CIRP, 2017, 58: 487–492.

[9] Zheng Bin, Xiong Jie Optimization design of bracket of profile measurement equipment based on ANSYS[J]. Manufacturing Automation, 2015, 37 (11): 130-132.

[10] Lou Yunge, Zhao Huiying, Yang Heqing, et al. Optimization Design of Welding Gantry Structure on Large Diameter Measuring Instrument[J]. Journal of Zhongyuan University of Technology, 2013, 24 (1): 1-4+51.

[11] Tian Xiaojie, Wang Zhen, Liu Duo, et al. Jack-up platform leg optimization by topology optimization algorithm-BESO[J]. Ocean Engineering, 2022, 257: 111633.

[12] Jia Dongsheng, Feng Pengcheng, Wang Liandi, et al. An Origami Shield with Supporting Frame Structures Optimized by A Feature-driven Topology Optimization Method[J]. Defence Technology, 2023: S2214914723000491.

[13] Sun Zhaoyou, Wang Yaguang, Gao Zhonghao, et al. Topology optimization of thin-walled structures with directional straight stiffeners[J]. Applied Mathematical Modelling, 2023, 113: 640–663.

[14] Wang Xucheng. Finite Element Method[M]. Beijing: Tsinghua University Press, 2003 (in Chinese).

[15] Su Hua, Chen Weijun, Gong Chunlin, et al. Oriented Topology Optimization of Thin-walled Structure with Circumferential Rib Enhancement of Stability[J]. Journal of Astronautics, 2022, 43 (3): 374-382.

[16] Long Haiqiang, Hu Yumei, Jin Xiaoqing, et al. An optimization procedure for spot-welded structures based on SIMP method[J]. Computational Materials Science, 2016, 117: 602–607.

[17] Xu Huayang, Guan Liwen, Wang Liping, et al. Topology Optimization for the Arm of Flight Simulator under Inertial Loads[J]. Journal of Mechanical Engineering, 2014, 50 (9): 14-23.

[18] Lakshmi Srinivas G, Javed Arshad. Topology optimization of rigid-links for industrial manipulator considering dynamic loading conditions[J]. Mechanism and Machine Theory, 2020, 153: 103979.